Form factor measurements with $\overline{\mathrm{P}}$ANDA at FAIR

E. Tomasi-Gustafsson

(on behalf of the $\overline{\mathrm{P}}$ANDA collaboration)

CEA,IRFU,SPhN, Saclay, 91191 Gif-sur-Yvette Cedex, France, and
CNRS/IN2P3, Institut de Physique Nucléaire, UMR 8608, 91406 Orsay, France

Abstract The high intensity and high energy antiproton beams which will be produced at FAIR open the possibility to determine time-like electromagnetic form factors in a wide kinematical range, through the annihilation reaction: $\mathrm{p}+\bar{\mathrm{p}}\to\mathrm{e}^{+}+\mathrm{e}^{-}$. The status of the proposed experiment as well as the expected results are presented on the basis of realistic simulations. The impact of these measurements on the understanding of the nucleon structure, of the asymptotic properties of form factors and of the reaction mechanism are discussed using model independent statements based on symmetry properties of the strong and electromagnetic interactions in connection with space-like data.

Key words electromagnetic form factors, antiprotons, nucleon structure, QCD

PACS 25.43.+t, 13.40.Gp

1 Introduction

The possibility to accelerate high energy and high intensity antiproton beams at the future facility $\overline{\mathrm{P}}$ANDA at FAIR [1] opens the possibility of new investigations in the domain of perturbative QCD. Proton-antiproton annihilation is a privileged tool to study gluonic excitations. The accessible hadronic states are not limited by the quantum number $J^{PC}=1^{--}$, as is the case with electron positron colliders. High statistics, particularly needed for the study of exotic systems, will be insured by the high luminosity of FAIR and high counting rate of the detector. Charmonium spectroscopy, hypernuclear physics, hadron in nuclear matter will be subjects of high precision investigations. Electromagnetic processes are also accessible by selecting final channels involving leptons. Here we focus on the annihilation process into an electron positron pair, which allows to access proton electromagnetic form factors in the time-like (TL) region.

Nucleon electromagnetic (EM) form factors (FFs) describe the dynamical properties, as the charge and magnetic distributions. Elastic EM FFs contain information on the hadron ground state. Assuming P and T invariance, the EM structure of a hadron of spin S is fully described by $2S+1$ FFs. The nucleon is described by two FFs, the Dirac F_1 and the Pauli F_2 FFs, or by a linear combination of them, the Sachs FFs: electric, G_{E} and magnetic, G_{M}. They are accessible experimentally and theoretically, which allows a straightforward test of nucleon models.

FFs have been object of studies since long time in the space-like (SL) region [2] through the Rosenbluth separation method in electron hadron elastic scattering, i.e., the measurement of the differential cross section at different angles, for the same value of momentum transfer squared, $Q^2 = -q^2$ [3]. In recent years, due to the development of high intensity, highly polarized electron beams, large acceptance spectrometers, polarized targets, and hadron polarimeters in the GeV range (or polarized targets) it has been possible to apply the polarization method, suggested already in 1967 by A.I. Akhiezer and M.P. Rekalo. In Ref. [4] it was shown that using longitudinally polarized electrons on a polarized target (or measuring the polarization of the outgoing proton in the scattering plane), an interference term appears in the polarized cross section, which is proportional to the product $G_{\mathrm{E}}G_{\mathrm{M}}$, and it is therefore more sensitive to a small contribution of G_{E}. This method has been recently applied by the GEP collaboration at the Jefferson Laboratory in a series of measurements, up to $Q^2 \sim 9~(\mathrm{GeV}/c)^2$ [5]. A larger precision was expected at large Q^2, where the magnetic contribution

to the cross section is dominant, but the real surprise was that the ratio of the electric to magnetic FF, more exactly $\mu G_{\rm E}/G_{\rm M}$ (μ is the magnetic moment of the proton) deviates from unity, contrary to what is found from Rosenbluth separation measurements. Both methods assume one photon exchange. This result gave rise to a number of theoretical papers and speculations. It is possibly related to radiative corrections, which appear to be very large for the cross section and are neglected in the polarization ratio.

In the TL region, FFs are accessible through the annihilation reactions $\bar{\rm p}+{\rm p}\leftrightarrow{\rm e}^+ +{\rm e}^-$. In this paper we discuss the perspectives opened by the antiproton beams at $\overline{\rm P}$ANDA , concerning the following aspects. Besides the determination of FFs ratio in a large kinematical domain, the large Q^2 values which can be achieved (up to ~ 25 (GeV/c)^2) allow to test the transition to pQCD and the pQCD predictions for the asymptotic behavior of FFs. Analyticity requirements also give important constraints, in this respect. Assuming crossing symmetry, the reaction mechanism is the same for the crossed reactions at the level of Born approximation. In the framework of one photon exchange mechanism, in the SL region the differential cross section is even in $\tan\theta_{\rm e}$ ($\theta_{\rm e}$ is the scattering angle of the electron in the laboratory system), whereas in TL region it is even in $\cos\theta$, where θ is the center of mass angle of the emitted electron

(or positron).

2   The $\overline{\rm P}$ANDA experiment

FAIR, Facility for Antiproton and Ion Research, is an international accelerator complex to be built in Darmstadt, as an extension of the existing GSI accelerator complex. It is designed for multipurpose research in nuclear and atomic physics. High intensity proton and ion beams will produce secondary beams. Storage rings will allow the simultaneous operation of up to five different experiments. Antiproton beams will be stored in the HESR (High Energy Storage Ring) and accelerated in the momentum range $1.5-15$ GeV/c. Two options are foreseen: high luminosity up to 2×10^{32} cm^{-2}s^{-1}, with momentum resolution $\Delta p/p = 10^{-4}$ or high resolution mode $\Delta p/p = 10^{-5}$ and lower luminosity.

The $\overline{\rm P}$ANDA detector is a 4π fixed target detector, designed to achieve momentum resolution at percent level for charged particles, high rate capability up to 10 MHz and good vertex resolution (100 μm). It consists of two magnetic spectrometers: the forward and the target spectrometers. The target spectrometer is surrounded by a 2 T superconducting solenoid. A 2 Tm dipole magnet analyzes the momentum of the charged particles emitted at polar angles smaller than 10°.
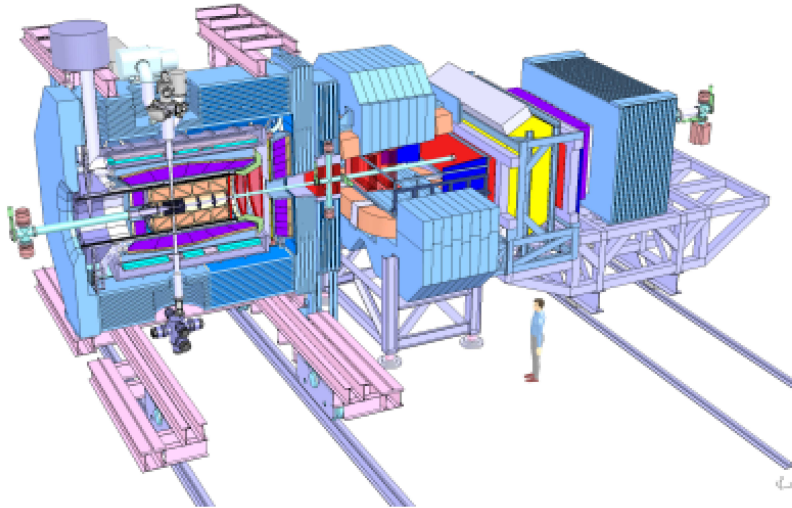

Fig. 1.   3D-view of the $\overline{\rm P}$ANDA detector.

Each spectrometer is equipped with detectors for tracking, charged particle identification, electromagnetic calorimetry and muon identification.

The internal target has to be installed in a limited space, in the ultra-high vacuum of the storage ring. The expected average luminosity $\mathcal{L}=1.6\cdot 10^{32}$ cm^{-2} s^{-1} will be reached with a pellet target of thickness $4\cdot 10^{15}$ hydrogen atoms/cm^2, and 10^{11} stored antipro-

tons in HESR.

The interaction point is reconstructed by a microvertex detector (MVD), consisting of layers of radiation hard silicon pixel detectors surrounded by silicon strip detectors. Straw tubes (STT) or a time projection chamber (TPC), with GEM detectors at forward angles complete the charged particle tracking and identification. The time of flight of particles emitted at large polar angles will be measured in a time of flight barrel. The electromagnetic calorimeter (based on PbWO4 crystals) will provide good energy and time resolution for the detection of photons and electrons at intermediate energy from a few MeV to $\simeq 10$ GeV. Detectors based on Cherenkov light (DIRC), which are very efficient for pion-electron separation for momentum $p < 1$ GeV/c, will be used in a barrel detector and a forward endcap detector.

For the identification of an electron pair in $\bar{\mathrm{p}}$p annihilation, particularly important are physical quantities such as momentum, ratio of energy loss to path length in each straw tube ($\mathrm{d}E/\mathrm{d}x$), Cerenkov angle in the DIRC detector, and the energy deposited in the electromagnetic calorimeter (EMC). In particular, EMC provides the ratio of the measured energy deposit to the reconstructed momentum. Electrons deposit all the energy in an electromagnetic shower, while muons and hadrons loose in average a much lower fraction of their kinetic energy.

The most important background for the reaction of interest is represented by hadronic reactions like the annihilation in two pions, with a cross section which is six order of magnitudes larger. To discriminate pions from electrons, severe cuts should be applied to the PID combined likelihood for the assumption that the detected particle is an electron. Realistic simulations, including acceptance and efficiency of the detector show that after applying such cuts together with kinematical selection, one can reach a background suppression factor of the order of few 10^9 in the angular range $|\cos(\theta)| < 0.8$ (see Refs. [1, 6]).

3   Time-like form factors with $\overline{\mathrm{P}}$ANDA

At $\overline{\mathrm{P}}$ANDA TL FFs will be accessible through the annihilation reaction:

$$\bar{\mathrm{p}} + \mathrm{p} \rightarrow \mathrm{e}^+ + \mathrm{e}^-. \qquad (1)$$

The differential cross section for the annihilation process (1) was first obtained in Ref. [7] and all the po-

larization observables were derived in [8, 9]:

$$\frac{\mathrm{d}\sigma}{\mathrm{d}(\cos\theta)} = \frac{\pi\alpha^2}{8M^2\tau\sqrt{\tau(\tau-1)}}[\tau|G_{\mathrm{M}}|^2(1+\cos^2\theta)+$$

$$|G_{\mathrm{E}}|^2\sin^2\theta], \ \tau = \frac{q^2}{4M^2}, \qquad (2)$$

where M is the proton mass. The linear dependence in $\cos^2\theta$ of Eq. (2) results directly from the assumption of one-photon exchange, where the spin of the photon is equal to one and the electromagnetic hadron interaction satisfies C invariance. Any deviation from linearity can be attributed to contributions beyond the Born approximation. Eq. (2) can be rewritten as a linear function of $\cos^2\theta$ [10]:

$$\frac{\mathrm{d}\sigma}{\mathrm{d}(\cos\theta)} = \sigma_0[1 + \mathcal{A}\cos^2\theta], \qquad (3)$$

in terms of the angular asymmetry $\mathcal{A}$:

$$\mathcal{A} = \frac{\tau|G_{\mathrm{M}}|^2 - |G_{\mathrm{E}}|^2}{\tau|G_{\mathrm{M}}|^2 + |G_{\mathrm{E}}|^2} = \frac{\tau - \mathcal{R}^2}{\tau + \mathcal{R}^2}, \ \mathcal{R} = \frac{|G_{\mathrm{E}}|}{|G_{\mathrm{M}}|}. \qquad (4)$$

σ_0 is the differential cross section at 90°:

$$\sigma_0 = \frac{\pi\alpha^2}{2q^2}\sqrt{\frac{\tau}{\tau-1}}\left(|G_{\mathrm{M}}|^2 + \frac{1}{\tau}|G_{\mathrm{E}}|^2\right). \qquad (5)$$

3.1   Determination of electric and magnetic form factors

We estimated the counting rates on the basis of a realistic parametrization of FFs, assuming the nominal luminosity. Simulations, including acceptance and efficiency, were done for reaction (1) in different kinematical conditions. For each q^2 value, the ratio $\mathcal{R}$ was determined from a two parameter fit to the reconstructed spectra for the differential cross section issued from the simulation procedure. The results are shown in Fig. 2, where the expected uncertainty on $\mathcal{R}$ is plotted as a function of q^2 as a yellow band for the case $\mathcal{R} = 1$, to be compared with the existing values from Refs [11]. (squares) and [12] (triangles). In the low q^2 region, the expected precision at $\overline{\mathrm{P}}$ANDA is at least one order of magnitude better than for the existing data and a meaningful value for $\mathcal{R}$ can be extracted up to at least $q^2 \sim 14$ (GeV/c)^2. Nucleon models are presently little constrained and predictions display a large dispersion, as shown in Fig. 2. As an example, three models originally built in the SL region have been analytically extended to the TL region [9], readjusting the parameters in order to fit the world data in all the kinematical region (i.e., in SL region, the electric and magnetic proton and neutron FFs, and in TL region, the magnetic FF of the proton and the few existing data for neutron).

A QCD inspired parametrization, based on scaling laws, predicts $\mathcal{R} = 1$, as it depends only on the number of constituent quarks (dashed line). The solid line is based on a vector meson dominance (VDM) approach, and grows up to $q^2 \sim 15$ $(\text{GeV}/c)^2$. The blue-dotted line is a prediction based on an extended VDM model which includes the proper asymptotic behavior predicted by QCD. Although these models reproduce reasonably well the FFs world data, they give different predictions for the form factor ratio and for all polarization observables.
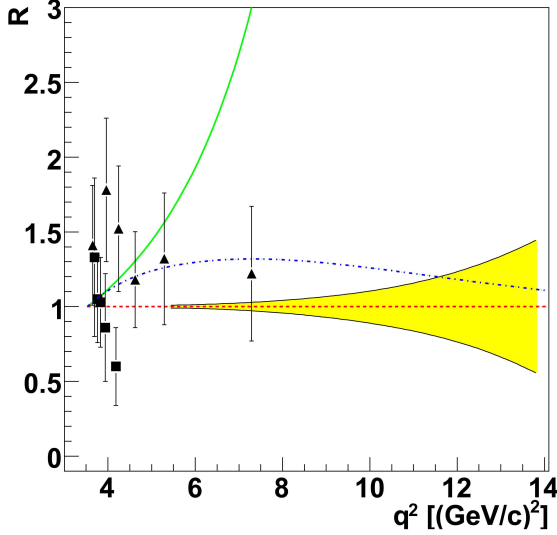

Fig. 2. Expected precision on the determination of the ratio $\mathcal{R}$, (yellow dashed band) as a function of q^2, compared with the existing data and to theoretical predictions.

With a precise knowledge of the luminosity, the absolute cross section can be measured up to $q^2 \sim 28$ $(\text{GeV}/c)^2$ allowing to extract a generalized FF, $|F_\text{P}|$. Comparing with the world data, one expects an improvement of at least a factor of ten.

3.2 The asymptotic region

The EM hadronic current is more simply parametrized in terms of the Dirac F_1 and Pauli F_2 FFs. PQCD predicts the asymptotic behavior $F_1 \sim Q^{-4}$ and $F_2 \sim Q^{-6}$ which is compatible with the Rosenbluth measurements, but not with polarization data, which suggest instead $F_2/F_1 \sim Q^{-1}$.

The values of G_M in the TL region, obtained under the assumption $|G_\text{E}| = |G_\text{M}|$, are larger than the corresponding SL values. A difference up to a factor of two in the absolute values in SL and TL regions can be seen also for other hadron FFs, including pions and neutrons, up to the largest value at which TL FFs have been measured. This has been considered

as a proof of the non applicability of the Phràgmen-Lindelöf theorem, or as an evidence that the asymptotic regime is not reached [8].

A general illustration of the world data for the proton form factors is given in Fig. 3, where proton FFs are shown as function of $|q^2|$, allowing a straightforward comparison in the whole kinematical region. In order to eliminate the steep q^4 dependence, all FFs are rescaled by the dipole function.

From top to bottom, one can see the generalized form factor, F_P (more exactly the magnetic proton FF under the assumption $|G_\text{E}| = |G_\text{M}|$) extracted from the total cross section in TL region, the magnetic proton FF in SL region which is obtained for $q^2 \geq 8.8$ $(\text{GeV}/c)^2$ under the assumption $|G_\text{E}| = 0$ (blue circles) and the electric FF in SL region. Two series of data clearly show the discrepancy between unpolarized (red triangles) and polarized (green stars) measurements.

The analyticity of FFs allows to apply the Phragmèn-Lindelöf theorem which gives a rigorous prescription for the asymptotic behavior of analytical functions, constraining FFs in TL and in SL regions to have the same value at large q^2:

$$\lim_{q^2 \to -\infty} F^{(\text{SL})}(q^2) = \lim_{q^2 \to \infty} F^{(\text{TL})}(q^2). \qquad (6)$$

This means that, asymptotically, FFs have the following constraints: - the imaginary part of FFs, in TL region, vanishes: $\text{Im } F_i(q^2) \to 0$, as $q^2 \to \infty$; - the real part of FFs, in TL region, coincides with the corresponding value in SL region, because FFs are real functions in SL region, due to the hermiticity of the corresponding electromagnetic Hamiltonian.

Unfortunately, this theorem does not indicate the physical value of q^2, starting from which it is valid at some level of precision. For this aim one needs some additional dynamical information. The assumption of the analyticity of FFs allows to connect the nucleon FFs in SL and in TL regions and to extend a parametrization of FFs available in one kinematical region to the other kinematical region. Dispersion relation approaches, which are based essentially on the analytical properties of nucleon electromagnetic FFs, can be considered as a powerful tool for the description of the q^2 behavior of FFs in the entire kinematical region as well as the quark-gluon string model.

For $\bar{\text{p}} + \text{p} \leftrightarrow \text{e}^+ + \text{e}^-$, in order to test asymptotic requirements, polarization data have to be known in addition to the differential cross section. T-odd polarization observables, which are determined by $\text{Im } F_1 F_2^*$, are especially interesting. The simplest of these observables is the P_y component of the proton polar-

ization in $e^+ + e^- \rightarrow \bar{p} = p$ which in general does not vanish, even in collisions of unpolarized leptons. Another is the asymmetry of leptons produced in $\bar{p}+p \rightarrow e^+ + e^-$, where one of the hadron is polarized normally to the scattering plane. These observables are especially sensitive to the different parametrizations of FFs, which suggest that the asymptotic region where the conditions of Phràgmen-Lindelöf theorem are satisfied, is reached at very large q^2 values, where present techniques do not allow measurements to be done [13].
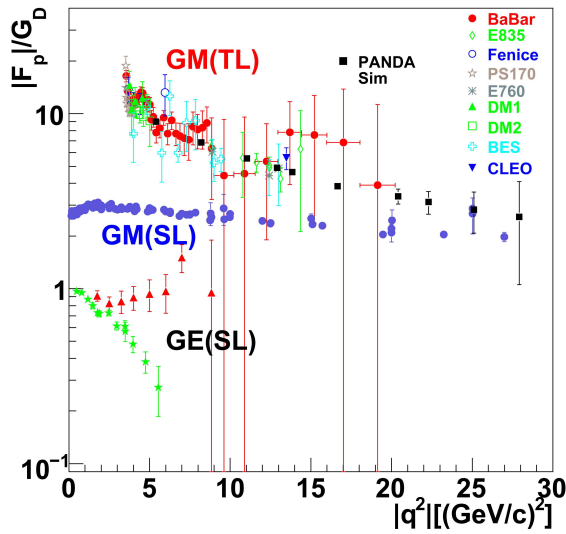

Fig. 3.   World data on proton form factors, in time and space-like regions, as functions of $|q^2|$, rescaled by dipole function. From top to bottom, magnetic FF in TL region including $\overline{\mathrm{P}}$ANDA simulated results (black solid squares), magnetic FF in SL region (blue circles), electric FF in SL region, from unpolarized (red triangles) and polarized (green stars) experiments. The expected errors for $\overline{\mathrm{P}}$ANDA (full black squares) correspond to an integrated luminosity of 2 fb^{-1}, which can be obtained in four months of data taking.

The expected precision of the future measurements with $\overline{\mathrm{P}}$ANDA (black solid squares) is shown in comparison with the existing data in Fig. 3. One can see that $\overline{\mathrm{P}}$ANDA will cover a large kinematical range and bring useful information with respect to the determination of the asymptotic region. The simulation has been performed using an extrapolation of FFs from the existing data. If such trend are proved to be realistic, $\overline{\mathrm{P}}$ANDA will reach the q^2 region where SL and TL data of the magnetic FF (which represents the dominant contribution) overlap. Note that there is no reason a priori that the electric and magnetic FF follow the same behavior and converge for

$q^2 \geq 25$ (GeV/c)^2.

3.3   The reaction mechanism

As stressed in the introduction, the expression of the cross section, Eq. (2), assumes one-photon exchange. In principle, the interaction can occur through two photon exchange (TPE). Although TPE is suppressed by a factor of α, it could play a role at large q^2, due to a possible enhancement from other mechanisms. It was suggested, that, if the transferred momentum is equally shared between the two virtual photons, the decrease of the cross section due to α counting could be partially compensated by the steep decrease of FFs with q^2. Recently, the possibility of a sizable TPE contribution has been discussed as possible solution to the discrepancies between experimental data, on elastic electron hadron scattering [5].

The model independent analysis of experimental observables taking into account the TPE contribution, for ep scattering and for the crossed annihilation channels can be found in Ref. [14–16]. The presence of TPE induces a more complicated spin structure of the matrix amplitude. In the scattering channel, instead of two real FFs, functions of one kinematical variable, q^2, one has to determine three amplitudes, complex functions of two kinematical variables, and the ϵ linearity of the Rosenbluth formula does not hold anymore. However, it is still possible to measure the real FFs, using electron and positron scattering on the proton in the same kinematical conditions, or measuring three T-odd or five T-even polarization observables. In the annihilation channel, the contribution of the one–photon–exchange diagram leads to an even function of $\cos\theta$, whereas the TPE contribution leads to four new terms reduced by an order of α with respect to the dominant contribution. At the reaction threshold where $q^2 = 4\,M^2$, one has $G_{\mathrm{M}} = G_{\mathrm{E}}$ and the differential cross section becomes independent on θ in the Born approximation. This is not anymore true in the presence of TPE terms. The terms of the cross section due to TPE are odd functions of $\cos\theta$. Therefore, they do not contribute to the differential cross section for $\theta = 90^0$.

The non linearity of the Rosenbluth fit in the scattering channel and the presence of odd $\cos\theta$ terms in the annihilation channel can be considered as model independent signatures of TPE (more exactly, of the real part of the interference between one and two photon exchange). Evidence of TPE, based on these signatures has not been found in the experimental data in the limit of their precision [17]. The present simulations show that the future $\overline{\mathrm{P}}$ANDA experiment will

be sensitive to a TPE contribution $\geq 5\%$ of the main (one photon) contribution [6].

Let us stress that the main advantage of the search of TPE in TL region is that the information is fully contained in the angular distribution. TPE effects cancel (are singled out) in the sum (difference) of the cross section at complementary angles, allowing to extract the moduli of the true FFs [15, 16]. TPE effects also cancel if one does not measure the charge of the outgoing lepton.

4   Conclusions

The FAIR accelerator complex and the $\overline{\text{P}}$ANDA detector will allow new test of perturbative QCD, and in particular the measurement of the proton form factors in a large kinematical domain where FFs are complex, through the annihilation channels $\bar{\text{p}}+\text{p} \leftrightarrow \text{e}^+ +\text{e}^-$. In the near future the knowledge of electromagnetic proton FFs will be extended in a wide kinematical region, allowing a unified description in both SL and TL regions. It will be possible to clarify both issues, the reaction mechanism and the proton electromagnetic structure at short distances. Moreover, the individual determination of FFs moduli will be possible in TL region, at least for moderate q^2 values. These data are expected to strongly constrain nucleon models. For $q^2 \geq 20$ $(\text{GeV}/c)^2$, where the electric contribution should become negligible, the validity of asymptotic properties predicted by QCD will be tested.

Due to crossing symmetry properties, the reaction mechanism should be the same in SL and TL

regions, at similar values of the transferred momentum. If TPE is the reason of the discrepancy between the polarized and unpolarized FFs measurements in SL region, a contribution of 5% is necessary to bring the data in agreement in the $|q^2|$ range between 1 and 6 $(\text{GeV}/c)^2$. Such level of contribution will be detectable in the $\overline{\text{P}}$ANDA experiment. In Ref. [18] the discrepancy has been attributed to the method of calculating radiative corrections. Radiative corrections are specific for each of these reactions, therefore a comparison of the data issued from the three channels, ep scattering, e^+e^- and $\bar{\text{p}}$p annihilation, will shed light on the reaction mechanism. Polarization would allow to access a larger set of observables. Single spin observables (in case of polarized beam or target) give information on the relative phase of FFs. The full determination of FFs requires at least the measurement of two spin observables. In case of absence of polarized beams, information on the phase of hadron FFs can be obtained for $\Lambda\bar{\Lambda}$ final state, which is self-polarizing through the weak decay $\Lambda \to \text{p}\pi^-$.

The same information can be accessed by the time reversed reaction $\text{e}^+ +\text{e}^- \to \bar{\text{p}}+\text{p}$ and BES3 can also bring important and complementary information: one can access in principle the neutron-antineutron final state and investigate the near threshold region where one expects a the contribution a possible $N\bar{N}$ bound state.

References

1   The $\overline{\text{P}}$ANDA collaboration. Physics Performance Report for $\overline{\text{P}}$ANDA : Strong Interaction Studies with Antiprotons. arXiv:0903.3905 [hep-ex]; http://www.gsi.de/PANDA; http://www.gsi.de/FAIR

2   Hofstadter R. Rev. Mod. Phys., 1956, **28**: 214–254

3   Rosenbluth M N. Phys. Rev., 1950, **79**: 615–619

4   Akhiezer A I, Rekalo M P. Sov. Phys. Dokl., 1968, **13**: 572–574; [Dokl. Akad. Nauk Ser. Fiz., 1968, **180**: 1081–1083]; Sov. J. Part. Nucl., 1974, **4**: 277–303; [Fiz. Elem. Chast. Atom. Yadra, 1973, **4**: 662–688]

5   Perdrisat C F, Punjabi V, Vanderhaeghen M. Prog. Part. Nucl. Phys., 2007, **59**: 694–764

6   Sudol M et al. arXiv:0907.4478 [nucl-ex], submitted to Eur. Phys. J. A

7   Zichichi A et al. Nuovo Cim., 1962, **24**: 170–180

8   Bilenky S M, Giunti C, Wataghin V Z. Phys. C, 1993, **59**: 475–480

9   Tomasi-Gustafsson E et al. Eur. Phys. J. A, 2005, **24**: 419–430

10 Tomasi-Gustafsson E, Rekalo M P. Phys. Lett. B, 2001, **504**: 291–295

11 Bardin G et al. Nucl. Phys. B, 1994, **411**: 3–32

12 Aubert B et al (BABAR collaboration). Phys. Rev. D, 2006, **73**: 012005

13 Tomasi-Gustafsson E, Gakh G I. Eur. Phys. J. A, 2005, **26**: 285–291

14 Rekalo M P, Tomasi-Gustafsson E. Eur. Phys. J. A, 2004 **22**: 331–336; Nucl. Phys. A, 2004, **740**: 271–286; Nucl. Phys. A, 2004, **742**: 322–334

15 Gakh G I, Tomasi-Gustafsson E. Nucl. Phys. A, 2006, **771**: 169–183

16 Gakh G I, Tomasi-Gustafsson E. Nucl. Phys. A, 2005, **761**: 120–131

17 Tomasi-Gustafsson E et al. Phys. Lett. B, 2008, **659**: 197–200

18 Bystritskiy Yu M, Kuraev E A, Tomasi-Gustafsson E. Phys. Rev. C, 2007, **75**: 015207